Sulfate ion in raw water affects performance of high-basicity PACl coagulants produced by $Al(OH)_3$ dissolution and base-titration: removal of SPAC particles by coagulation-flocculation, sedimentation, and sand filtration

Yize Chen [a], Yoshifumi Nakazawa [a], Yoshihiko Matsui [b, *], Nobutaka Shirasaki [b], Taku Matsushita [b]

[a] Graduate School of Engineering, Hokkaido University.
N13W8 Sapporo 060-8628 Japan

[b] Faculty of Engineering, Hokkaido University
N13W8 Sapporo 060-8628 Japan

* Corresponding author. Phone: +81-11-706-7280.
E-mail address: matsui@eng.hokudai.ac.jp (Y. Matsui)

ABSTRACT

Many PACl (poly-aluminum chloride) coagulants with different characteristics have been trial-produced in laboratories and commercially produced, but the selection of a proper PACl still requires empirical information and field testing. Even PACls with the same property sometimes show different coagulation performances. In this study, we compared PACls produced by $AlCl_3$-titration and $Al(OH)_3$-dissolution on their performance during coagulation-flocculation, sedimentation, and sand filtration (CSF) processes. The removal targets were particles of superfine powdered activated carbon (SPAC), which are used for efficient adsorptive removal of micropollutants, but strict removal of SPAC is required because of the high risk of their leakage after CSF. PACls of high-basicity produced by $AlCl_3$-titration and $Al(OH)_3$-dissolution were the same in terms of the ferron assay and colloid charge, but their performance in CSF were completely different. High-basicity $Al(OH)_3$-dissolution PACls formed large floc particles and yielded very few remaining SPAC particles in the filtrate, whereas high-basicity $AlCl_3$-titration PACls did not form large floc particles. High-basicity PACls produced by $Al(OH)_3$-dissolution were superior to low-basicity PACl in lowering remaining SPAC particles by the same method because of their high charge neutralization capacity, although their floc formation ability was similar or slightly inferior. However, high-basicity $Al(OH)_3$-dissolution PACl was inferior when the sulfate ion concentration in the raw water was low. Sulfate ions were required in the raw water for high-basicity PACls to be effective in floc formation. In particular, very high sulfate concentrations were required for high-basicity $AlCl_3$-titration PACls. The rate of hydrolysis, which is related to the polymerization of aluminum species, is a key property, besides charge neutralization capacity, for proper coagulation, including

formation of large floc particles. The aluminum species in the high-basicity PACls, in particular that produced by $AlCl_3$-titration, was resistant to hydrolysis, but sulfate ions in raw water accelerated the rate of hydrolysis and thereby facilitated floc formation. Normal-basicity $Al(OH)_3$-dissolution PACl was hydrolysis-prone, even without sulfate ions. Aluminum species in the high-basicity $AlCl_3$-titration PACl were mostly those with a molecular weight (MW) of 1–10 kDa, whereas those of high-basicity $Al(OH)_3$-dissolution PACls were mostly characterized by a MW >10 kDa. Normal-basicity $Al(OH)_3$-dissolution PACl was the least polymerized and contained monomeric species.

Keywords: hydrolysis; ferron; basicity; floc; PACl

1. Introduction

With the recent development of milling technology, it is possible to produce superfine powdered activated carbon (SPAC) by micro-milling conventionally sized PAC (powdered activated carbon) to a mean diameter of ~1 μm (Matsui et al., 2004, 2013b). The larger adsorption capacity and faster adsorption kinetics of SPAC compared with PAC lead to superior adsorptive removal of organic pollutants from water by SPAC (Ando et al., 2010; Bonvin et al., 2016; Matsui et al., 2015, 2012; Partlan et al., 2016). These advantages of SPAC have led to the expectation that it will be used in water and wastewater treatment (Bonvin et al., 2016). However, there is a concern that the risk of leakage from the treatment process may be higher for SPAC than for conventionally sized PAC. The application of high-basicity (basicity 70%) PACl (polyaluminum chloride) coagulant instead of normal-basicity PACl coagulant has been proposed as an effective way to minimize the loss of SPAC particles during the CSF (coagulation-flocculation, sedimentation, and sand filtration) process, but not all types of high-basicity PACls are effective coagulants (Nakazawa et al., 2018a). The reason is not yet clear.

In Japan, the country where PACl was invented, high-basicity PACl is rapidly becoming a popular replacement for normal basicity coagulant (50%) because use of high-basicity PACl results in lower aluminum residuality in treated water and higher removal efficiencies of natural organic matter (NOM). Furthermore, high-basicity PACl has a greater ability to attenuate transmembrane pressure rise when it is applied in coagulation pretreatment before membrane microfiltration, and storage of high-basicity PACl for a long time does not result in aluminum hydroxide precipitation (Kimura et al., 2015, 2013). However, high-basicity PACl sometimes fails to outperform normal-basicity

PACl (personal communication, Taki Chemical Co., Ltd., 2019).

High-basicity and normal-basicity PACls are commercially produced by the $Al(OH)_3$-dissolution method. However, PACls produced by base-titration methods have been intensively studied in laboratory coagulation experiments, and satisfactory coagulation performance has been reported based on the residual turbidity after sedimentation (Chu et al., 2008; Gao and Yue, 2005). However, Nakazawa et al. (2018a) have reported that high-basicity PACls produced by $Al(OH)_3$-dissolution and by $AlCl_3$-titration perform very differently, although they are identical in terms of aluminum species based on the ferron assay (Wang et al., 2002). The former was very effective, but the latter was ineffective in forming large floc particles. Use of the latter resulted in a high concentration of residual SPAC particles in treated water. Overall, the evaluations of base-titration PACls have not been consistent. Even when water has been treated with several types of $Al(OH)_3$-dissolution PACl coagulants, the performance of the PACls has generally been specific to the raw water. The mechanisms responsible for this specificity have not been fully investigated and are not yet clearly understood.

One possibility is that PACl performance depends on the concentrations of inorganic ions as well as the concentrations of suspended particles and NOM in the raw water. The alkalinity of the raw water is believed to affect the efficiency with which turbidity and particles are removed by PACl coagulation because the aluminum ions in the PACl must undergo hydrolysis to become species that can effect coagulation, and the hydrolysis allows protons to react with alkalinity (Ye et al., 2007). Multivalent ions such as the sulfate ion, which is commonly found in raw water, are also thought to influence coagulation because they destabilize positively charged aluminum polynuclear species (Letterman and Yiacoumi, 2010). However, the effects of sulfate ions have not been

105 sufficiently studied. Sricharoenchaikit and Letterman (1987) have reported that sulfate
106 ions influence the flocculation kinetics of a polystyrene suspension destabilized by
107 aluminum nitrate. Wang et al. (2002) focused on the effect of the sulfate ion in $AlCl_3$-
108 titration PACl coagulants but not on the sulfate ions in raw water.
109 Moreover, most of the foregoing studies of PACl coagulation have used PACls
110 prepared by the $AlCl_3$-titration method, but the characteristics and coagulation
111 performances of PACls produced by the $Al(OH)_3$-dissolution method, which is quite
112 popular in PACl-production industries, have seldom been studied. Experimental results
113 of a series of CSF processes, rather than of jar tests, are still not enough for PACl
114 coagulants.
115 In this study, we measured the concentrations of residual SPAC particles after the CSF
116 process as well as the flocculation-sedimentation characteristics of SPAC particles with
117 the following two objectives. The first objective was to investigate the coagulation
118 characteristics of high-basicity PACls produced by two methods: $Al(OH)_3$-dissolution and
119 $AlCl_3$-titration. The second objective was to investigate the effects of sulfate ions in the
120 raw water.
121
122 **2. Materials & methods**
123
124 *2.1 Coagulants*
125 Three kinds of PACls were used in this study. Among them, PACl-70d (basicity 70%)
126 and PACl-50d (basicity 50%) ("d" represents "dissolution") are commercially available
127 PACls and were provided by Taki Chemical Co., Ltd. (Hyogo. Japan), which produced
128 them by dissolving $Al(OH)_3$ in HCl and H_2SO_4 [as described in Sato and Matsuda (2009)].

Briefly, a mixture of $AlCl_3$, $Al_2(SO_4)_3$, and $Al(OH)_3$ was heated to obtain a solution with a basicity of 50% ($Al(OH)_3$-dissolution method). The basicity was then raised to 70% at <85 °C by adding a solution of sodium carbonate. The third kind of PACl used, PACl-70t ("t" represents "titration"), was produced in the authors' laboratory by titrating a NaOH solution into an $AlCl_3$ solution. The procedure, which is called the $AlCl_3$-titration method, consists of the following steps. A NaOH solution (1 mol/L; Kanto Chemical Co., Inc., Tokyo, Japan) is diluted with ultrapure water (Milli-Q water) produced by an ultrapure lab water system (Milli-Q Advantage; Merck KGaA, Darmstadt, Germany) to a concentration of 0.26 mol/L. Then, $AlCl_3 \cdot 6H_2O$ and $Al_2(SO_4)_3 \cdot 16H_2O$ (FUJIFILM Wako Pure Chemical Corporation) are dissolved to obtain 80 mL of a 0.5-M Al solution. A pump and tubes are prepared for titrating the NaOH solution with the Al solution. After the NaOH solution and Al solution are heated to 50–60 °C and 85–90 °C, respectively, the titration is started. The flow rate of the NaOH solution is set at 4 mL/min to avoid the appearance of a precipitate during the titration. After the titration is finished, the resultant solution is preserved in a refrigerator at 4 °C for one night and then heated at 90–95 °C for 3 hours. After the temperature has returned to room temperature, the solution is preserved at 4 °C until the time of the experiment. Table 1S (SI) lists the basic properties of the PACl coagulants. During the experiment, PACls from the stock were first diluted to 0.1 mol-Al/L using Milli-Q water. The dosage of PACl coagulant was 2.5 mg-Al/L unless otherwise noted.

2.2 Superfine powdered activated carbon (SPAC)

A commercially available wood-based PAC (Taiko W) was obtained from Futamura Chemical Co., Ltd. (Nagoya, Japan) and was milled with a bead mill (LMZ015; Ashizawa

153 Finetech, Ltd., Chiba, Japan) to produce a SPAC. The details of the procedure are
154 described elsewhere (Pan et al., 2017).
155
156 *2.3 Water*
157 Three kinds of water (C, E, and J series) were prepared (Table 1). Water of the C series
158 was prepared from natural water (designated as C0) that was sampled from the Chibaberi
159 River (Rumoi City, Hokkaido, Japan). Water C0 was diluted with pure water (Elix water,
160 Elix Advantage; Merck KGaA, Darmstadt, Germany), and its ion concentrations were
161 adjusted by adding $NaHCO_3$ or Na_2SO_4 (FUJIFILM Wako Pure Chemical Corporation)
162 to prepare Waters C1 and C2. Waters of the E series (E1–7) were ionic waters prepared
163 by adding $MgSO_4$, $CaCl_2$, HNO_3, KOH, Na_2SO_4, and $NaHCO_3$ to Elix water. There were
164 two waters in the J series: water sampled from the Joganji River (Toyama, Japan) and the
165 same water adjusted by addition of Na_2SO_4. Alkalinity, which might affect the coagulation,
166 was adjusted at each constant for C2–3, E1–7, and J1–2 waters. These waters were stored
167 at 4 °C. The waters were ready for a PACl hydrolysis test after their temperatures had
168 returned to room temperature (~20 °C). The waters were ready for CSF experiments after
169 their temperatures had returned to room temperature and SPAC (the target for removal)
170 had been added at a concentration 2 mg/L. Concentrations of ions in the water were
171 measured by ion chromatography (ICS-1000 and ICS-1100; Thermo Scientific, Bremen,
172 Germany). The alkalinity was measured by titrating the water with 0.01 M H_2SO_4. For
173 the measurement of dissolved organic carbon (DOC), the water sample was filtered
174 through a membrane filter (0.45-μm pore size; Toyo Roshi Kaisha, Ltd., Tokyo, Japan),
175 and the DOC was then measured with a TOC analyzer (TOC900; GE Analytical
176 Instruments, Inc., Boulder, CO, USA).

177

178 *2.4 Characterization of PACl coagulants*

179 The ferron assay was conducted with the 3 PACls. Immediately after being diluted
180 with Milli-Q water to a concentration of 0.1 mol-Al/L, the PACls were added to the ferron
181 reagent (8-hydroxy-7-indo-5-quinoline sulfonic acid; FUJIFILM Wako Pure Chemical
182 Corporation) to initiate the reaction. The absorbance at 366 nm was then measured using
183 an ultraviolet light meter (UV-1800; Shimadzu, Kyoto, Japan). Dilution of the PACls was
184 acceptable because dilution has little effect on the distribution of ferron (Kimura et al.,
185 2013; Wang et al., 2002). The aluminum species in the PACl were divided based on their
186 reaction time with the ferron reagent into Ala (monomeric species, within 30 s), Alb
187 (polymeric species, from 30 s to 120 min), and Alc (colloidal species, did not react within
188 120 min) (Wang et al., 2004; Yan et al., 2007).

189 The colloid charges of the PACls were measured via colloid titration. A PACl was
190 diluted with Milli-Q water into 0.1 mol-Al/L and was titrated with a potassium polyvinyl
191 sulfate titration solution (N/400, for colloidal titration; FUJIFILM Wako Pure Chemical
192 Corporation) using an automatic titrator (COM-555; Hiranuma Sangyo Co., Inc., Ibaraki,
193 Japan) (Matsui et al., 2017).

194 For the ESI-MS analyses, PACls were diluted to a concentration of 0.1 mol-Al/L and
195 introduced into an Orbitrap LC-MS system (Exactive; Thermo scientific, Bremen,
196 Germany) under the following conditions: scan range m/z 200–2000; spray voltage 3.0
197 kV; capillary temperature 300 °C; capillary voltage 32.5 V; heater temperature 250 °C.
198 Peaks and the possible formulas of aluminum species were calculated by Xcalibur 2.2
199 (Thermo Fisher Scientific).

200 ^{27}Al-NMR analysis was conducted with a JNM-ECA Series FT NMR (ECA 600;

JEOL Ltd., Tokyo, Japan). $NaAl(OH)_4$ (FUJIFILM Wako Pure Chemical Corporation) solution (0.01 mol-Al/L) was used as the internal standard. $AlCl_3$ (FUJIFILM Wako Pure Chemical Corporation) solution (0.1 mol-Al/L) was used as the reference material. Parameters for the measurement were as follows: field strength, 14.09 T; frequency, 78247 Hz; resonance frequency, 156.39 MHz; number of scans, 8000; temperature 70 °C. The data and peaks were processed with the data-processing software provided with Nakamura (2009).

The molecular weight (MW) distributions of aluminum species were measured by using membrane filters with nominal MW cutoffs of 1 and 10 kDa (regenerated cellulose membrane, Ultracel PL; Merck KGaA, Darmstadt, Germany). The membrane filters were set in 50-mL stirred cells (Amicon 8050 series; Merck KGaA, Darmstadt, Germany). Coagulants with concentrations higher than 0.1 mol-Al/L were diluted to 0.1 mol-Al/L using Milli-Q water in the stirred cell. The filtration was then started by applying 0.5-MPa pressure at 30 s after dilution. The filtration continued until 2 mL of filtrate had been collected from the 50-mL sample. The aluminum concentrations in the filtrates were measured with an inductively coupled plasma mass spectrometer (ICPMS, 7700x; Agilent Technologies, Inc., Santa Clara, CA, USA).

The following procedure was used to determine the rate of hydrolysis of the aluminum species in PACl. E-series water was placed in a 1-L rectangular plastic beaker. HCl or NaOH (0.1N) was added to bring the final pH to 7, and then PACl was added so that the concentration of aluminum was 2.5 mg/L. The solution was mixed at a G value (velocity gradient) of 600 s^{-1} for 40 s and then at a G value of 50 s^{-1} for 80 s. Ten-milliliter samples of water were taken at times of 15 s, 30 s, 60 s, and 120 s after the PACl injection. A portion of the sample was immediately filtered through a polytetrafluoroethylene (PTFE)

membrane (Φ47 mm; Merck KGaA, Darmstadt, Germany) with a pore size of 0.1, 1, or 10 μm. A PTFE membrane was used in this experiment because PTFE membranes have been reported to have the lowest tendency to adsorb aluminum (Matsui et al., 2013a). The Al concentration in the filtrate was measured by ICPMS.

2.5 Coagulation-flocculation, sedimentation, and rapid sand filtration (CSF) experiment

CSF experiments were used to evaluate the coagulation performances of the PACls. Four liters of raw water were placed in a rectangular plastic beaker. A predetermined volume of HCl or NaOH (0.1N) was added to the water to adjust the coagulation pH to 7.0. After 30 min of mixing, PACl was added. Rapid mixing conducted at a *G* value of 600 s^{-1} for 40 s was followed by three stages of slow mixing at *G* values (in chronological order) of 50 s^{-1} for 170 s, 20 s^{-1} for 170 s, and 10 s^{-1} for 320 s, respectively. The total *GT* value for the rapid and slow mixing was 39,100. After mixing, the water was allowed to stand for 1 hour for sedimentation. The supernatant was then transferred at a constant rate to the sand-filtration column for sand filtration. Sand filtration was conducted at a rate of 90-m/d with a 50-cm–deep column containing sand (effective diameter, 0.6 mm; uniformity, 1.3). Filtrate was collected from 13 to 40 min after the start of filtration. After the filtration was finished, the sand filter was backwashed with tap water and then forward washed with Milli-Q water.

The Zeta potentials of the water before coagulation, the water after rapid mixing, and the supernatant were measured with a Zeta potential meter (Zetasizer Nano ZS; Malvern Panalytical Ltd., Almelo, Netherlands) using a dip cell. The turbidity of the water before coagulation, the supernatant, and the sand filtrate were measured with a turbidity meter (2100Q portable turbidimeter; Hach Company, Loveland, CO, USA). Formation of floc

249 particles was evaluated based on pictures of the beaker taken with a DSLR (digital single
250 lens reflex) camera (EOS 60D; Canon Ltd., Tokyo, Japan) at the end of rapid mixing and
251 during slow mixing.
252
253 *2.6. Membrane filtration and image analysis*
254 The carbon particles that remained in the sand filtrate were enumerated via membrane
255 filtration and image analysis. The details of this method have been described by
256 Nakazawa et al. (2018b) but can be briefly described as follows. Sample water was
257 filtered through a membrane filter (pore size 0.1 μm, PTFE, Φ25 mm; Merck KGaA), and
258 then the filter was allowed to dry under natural conditions. Photographs of the filter were
259 taken with a microscope (VHX-2000; Keyence corporation, Osaka, Japan), and the SPAC
260 particles on the photographs were counted with the software built into the microscope.
261
262 **3. Results and discussion**
263
264 *3.1 Characteristics of PACl coagulants*
265 As shown in Fig. 1 (Panel A), the ferron distributions of PACl-70t and PACl-70d were
266 almost the same: Alc species accounted for more than 65% of total aluminum, Alb for
267 ~15%, and Ala for ~20%. Among the three PACls, the percentage of Ala was highest
268 (40%) in PACl-50d. The similarity of the charge neutralization abilities of PACl-70t and
269 PACl-70d (Fig. 1 (Panel B)) reflected the similarities of their ferron distributions. The
270 fact that the charge neutralization ability was smaller for PACl-50d than for PACl-70t and
271 PACl-70d reflected the lower percentage in PACl-50d of Alc + Alb (aluminum colloid
272 and polymer), which are generally regarded as the aluminum species with high charge

neutralization capacity (Yan et al., 2008).

Marked differences between the three PACls were observed in the MW distributions determined by membrane filtration (Panel C of Fig. 1). PACl-70t contained a relatively large amount of polymerized aluminum species with MWs ranging from 1 to 10 kDa compared with PACl-70d. PACl-50d contained a relatively large amount of aluminum species with low MWs (<1 kDa), which should include Al monomers. Differences were also observed in the ESI-MS spectrum of the three PACls (Fig. 1S, SI), although the formulas of the aluminum species could not be identified.

The ^{27}Al-NMR analysis spectra are shown in Fig. 1 (Panel D). The peak at $\delta = 0$ ppm, which is the indication of an Al monomer, was observed for all three PACls, but the fact that it was relatively high in the PACl-50d spectrum compared with the other spectra was consistent with the ferron assay results. A peak at $\delta = 62.5$ ppm is assigned to tetrahedrally coordinated Al in the Keggin Al_{13} structure ($Al(O)_4$) and is related to the presence of an e-Al_{13} polycation (Allouche et al., 2002; Sposito, 1995). This peak was found in all three PACl coagulants and was relatively intense in PACl-70d. The Keggin-type e-Al_{13} polycation is considered to be equivalent to Alb (Chen et al., 2007; Parker and Bertsch, 1992; Sposito, 1995), but this equivalence was not supported by the data of the present study: the percentages of Alb were similar in PACl-70d and PACl-70t and relatively small in PACl-50d. The broad resonance observed at $\delta = 10$–12 ppm in PACl-70t and PACl-70d (but not in PACl-50d) was assigned to octahedral aluminum sites [$Al(O)_6$] in oligomers (Casey, 2006; Tang et al., 2015). The larger area and higher intensity of the resonance at $\delta = 10$–12 ppm in PACl-70t versus PACl-70d meant that the amount of $Al(O)_6$ oligomer was higher in PACl-70t than in PACl-70d. The broad resonance at $\delta = \sim 70$ ppm, which is an indication of a Keggin-type δ-Al_{30} polycation, was not observed. PACl-70t and PACl-

297 70d therefore differed with respect to their aluminum species, although the ferron analysis
298 could not distinguish this difference. Finally, the three PACls were different.
299
300 *3.2 Comparison of PACls in CSF experiments*
301 The turbidity and residual SPAC particles during the CSF experiments are shown in
302 Fig. 2 (Panels A and B) and Fig. 2S (SI) for Waters C1 and E4, respectively. Turbidities
303 in the supernatant after sedimentation were very low when either PACl-70d or PACl-50d
304 was used to treat the water, and the turbidities in the sand filtrate after the rapid filtration
305 process reached an even lower level (Fig. 2S, SI). In contrast, use of PACl-70t resulted in
306 a relatively high residual turbidity in the supernatant for Water C1 (Panel A of Fig. 2) and
307 so little turbidity removal after sedimentation for Water E4 (Fig. 2S, SI) that we could not
308 conduct a sand-filtration experiment. Photographs taken during the coagulation-
309 flocculation process are shown in Fig. 2 (Panel C) and Fig. 3S (SI). At the end of slow
310 mixing, the floc size was very small when PACl-70t was used. In contrast, relatively large
311 floc particles were observed for both PACl-50d and PACl-70d. Although the rate of floc
312 formation seemed higher for PACl-50d because of the greater number of micro-floc
313 particles that were clearly observed at the end of rapid mixing, the residual SPAC particles
314 in the sand filtrate when PACl-50d was used was at the same level or higher versus PACl-
315 70d (Fig. 2 (Panel B, Fig. 2S, SI). Although PACl-50d was superior in terms of floc
316 formation, this superiority did not lead to lower numbers of residual SPAC particles in
317 the sand filtrate because of the low charge-neutralization ability of the PACl-50d, which
318 was apparent from the results of the ferron assay and colloid charge (Panels A and B of
319 Fig. 1). Nakazawa et al. (2018a and 2018b) have revealed that particles with un-
320 neutralized charge leak through CSF processes, and high-basicity PACls have a high

charge-neutralizing capacity.

The performance of PACl-70d and PACl-70t differed to a great extent, although they had nearly the same ferron distribution and colloid charge. The zeta potentials during coagulation using PACl-70d and 70t are shown in Fig. 4S (SI). The higher charge neutralization ability of PACl-70t versus PACl-70d has also been reported by Nakazawa et al. (2018a). The fact that the zeta potential of particles became close to zero after coagulation by PACl-70t meant that charge neutralization progressed well. However, floc formation was much slower with PACl-70t than with PACl-70d. The reason might be the difference in the aluminum species in the PACls, a difference that was seen in the MW distributions and ESI-MS and that was faintly apparent in the ^{27}Al-NMR spectra. The difference, however, was not reflected in the ferron species distribution (Ala, Alb, and Alc) and colloid charge (see section 3.1). Feng et al. (2007) have differentiated Alb (polymeric aluminum species) into two fractions: the faster-reacting polymers and the slower-reacting polymers. However, the main aluminum species in PACl-70d and PACl-70t was Alc (colloid aluminum species), not Alb. The large difference in coagulation performance between PACl-70d and PACl-70t may therefore not be attributable to the difference in the polymeric aluminum species (Alb). The colloid aluminum species (Alc) may include a variety of species with very different reaction rates. Such species differences were observed in the MW distributions and ESI-MS.

Aluminum coagulants, including PACls, are hydrolyzing aluminum salt coagulants. The aluminum species in PACl react with alkalinity after it is dosed to water, and the unstable aluminum hydroxide that is finally formed plays an important role in sweep coagulation (Letterman and Yiacoumi, 2010). In this study, we evaluated the speed of aluminum hydrolysis by measuring the concentrations of aluminum after filtration

through membranes of different pore sizes (0.1, 1, and 10 μm, Fig. 3). The rapid hydrolysis of PACl-70d and PACl-50d resulted in the most large (>10 μm) Al particles within 15 s after the PACl was injected into the water. The PACl-70t hydrolyzed at a much slower rate: more than half of the Al particles were still <10 μm in size 60 s after injection. The very different rates of hydrolysis of PACl-70t and PACl-70d may have reflected differences in the aluminum species that were observed in the MW distributions and ESI-MS. The difference of coagulation performance could not be explained solely on the basis of charge neutralization ability. Hydrolysis, which can be evaluated with a hydrolysis test, also plays an important role in coagulation performance.

3.3 Effect of sulfate ion in water

3.3.1 Effect of sulfate ion on CSF performance.

The sulfate ion in PACl is known to change the characteristics of the PACl (Nakazawa et al., 2018a). However, PACl-70t and PACl-70d had the same sulfate ion content, and therefore the sulfate ions in the PACls could not have caused a large difference in their coagulation performance. We then focused on the sulfate ions in the raw water. The effect of the sulfate ions was first investigated by using adjusted natural waters (C1 and C2) with different sulfate concentrations. There was no obvious difference in turbidity and removal of SPAC particles between sulfate concentrations of 15.9 mg/L and 6.4 mg/L (Fig. 5S, SI). However, the slower rate of formation of floc at 6.4 mg/L than at 15.9 mg/L (Fig. 4) suggested that there was a sulfate effect.

We further investigated the effect of sulfate ions by preparing artificial raw waters with various SO_4^{2-} concentration (E1–7 in Table 1). Fig. 5 shows the rates of turbidity removal by PACl-70t, PACl-70d, and PACl-50d. As the concentration of the SO_4^{2-} ion in

369 the raw water decreased, the removal of turbidity by PACl-70t and PACl-70d in
370 sedimentation supernatant decreased dramatically. In the absence of SO_4^{2-}, there was
371 almost no turbidity removal. Compared with PACl-70d and PACl-70t, on the other hand,
372 treatment with PACl-50d resulted in high turbidity removal, regardless of the SO_4^{2-} ion
373 concentration in the water. Even when the SO_4^{2-} concentration was zero, PACl-50d
374 produced supernatant with a low residual turbidity that was comparable to the turbidity
375 attained with 15.8-mg/L SO_4^{2-}. Photographs of floc formation were consistent with this
376 result (Fig. 6). When PACl-50d was used to treat the water, visible floc particles were
377 observed at the rapid-mixing stage when the water contained SO_4^{2-} at 3.5–15.8 mg/L, and
378 during the first stage of slow mixing, visible floc particles were also observed, even when
379 the water contained no SO_4^{2-} ions (Fig. 8S, SI). For PACl-70d, however, the rate of floc
380 formation slowed as the sulfate ion concentration decreased. When the SO_4^{2-}
381 concentration was 3.5 mg/L, visible floc particles were not formed during the rapid-
382 mixing stage; instead, they were formed only after slow mixing. At a SO_4^{2-} concentration
383 of zero, floc particles were not formed at all. At low sulfate concentrations, the floc
384 formation ability was therefore stronger for PACl-50d than for PACl-70d. PACl-70t
385 required a very high sulfate ion concentration (48.8 mg-SO_4^{2-}/L) for floc formation, but
386 even at such a high sulfate ion concentration, large floc particles did not form.
387 The sulfate ion in PACl is known to enhance the precipitation of aluminum ions in
388 water (De Hek et al., 1978). All commercially available PACls in Japan contain sulfate
389 ions, but JIS (Japanese Industrial Standards) standard JIS K 1475-1996 stipulates that the
390 sulfate ion content of PACl should be lower than 3.5% (Japanese Industrial Standards
391 Committee, 1996). The sulfate contents of PACl-70d and PACl-50d were 2% and 3%,
392 respectively. The unsatisfactory performance of PACl-70d at low SO_4^{2-} concentrations

might have resulted from its relatively low sulfate content. In order to test this hypothesis, Fig. 5 was redrawn using the total sulfate ion concentration (sulfate ion concertation in raw water plus sulfate ion added with the PACl) as the independent variable (Fig. 9S, SI). The total sulfate ion concentration did not explain the difference in the coagulation performances of PACl-70d and PACl-50d. Moreover, when PACl-70t and PACl-70d were compared, the requirement for sulfate ions was larger for PACl-70t than for PACl-70d, although the two PACls had the same sulfate content. Nakazawa et al. (2018a) have prepared a set of high-basicity PACl coagulants prepared by the $Al(OH)_3$-dissolution method and have reported that SPAC particle removal ability via PACl coagulation depends little on SO_4^{2-}/Al ratios in the range 0.11–0.15. These results indicate that the requirement of PACl-70d for sulfate ions in raw water is not related to its low sulfate content.

A dependence of PACl-70d coagulation on SO_4^{2-} concentrations in water was also observed in the concentrations of residual SPAC particles after CSF (Fig. 7). When SO_4^{2-} concentrations were at a low level of 3.5 mg/L, the residual SPAC particle concentration was quite high, 1790 particles/mL, a concentration that was higher than the concentration of 345 particles/mL achieved with PACl-50d at the same SO_4^{2-} concentration. At a SO_4^{2-} concentration of zero, residual SPAC particles were too numerous to count. Nakazawa et al. (2018a) have observed the superiority of PACl-70d over PACl-50d in reducing residual SPAC particles in water containing SO_4^{2-} at a concentration of 16 mg/L, and this trend was also observed in our study when the SO_4^{2-} concentration exceeded 6.4 mg/L. Our results show, however, that at relatively low SO_4^{2-} concentrations, normal-basicity PACl is superior to high-basicity PACl.

The effect of sulfate ions was further confirmed by the experiments using natural

417 water and SO_4^{2-}-adjusted natural water. For PACl-70d, floc did not form during the
418 mixing process (Panel A of Fig. 8), and the result was high residual turbidity in the
419 supernatant (Panel B of Fig. 8). With the increase of the sulfate ion concentration in the
420 water, the coagulation performance improved: formation of large floc particles was
421 observed, and turbidity in the supernatant became satisfactorily low. In contrast, the
422 performance of PACl-50d was fairly good, regardless of whether or not there was an
423 increase of the SO_4^{2-} concentration (Fig. 8). Our results showed that PACl-70d, which is
424 superior in reducing residual SPAC particles after CSF, requires a certain concentration
425 of SO_4^{2-} in the raw water to work efficiently.
426 *3.3.2 Effect of sulfate ion on PACl hydrolysis.*
427 The rates of hydrolysis of PACl-70t, 70d, and 50d at different sulfate concentrations
428 were investigated, and the results are shown in Fig. 9. There was little effect of sulfate
429 ions on the rate of hydrolysis for PACl-50d: the aluminum species in PACl-50 grew larger
430 than 10 μm within 15 s, no matter what the sulfate concentration in the water was. In
431 contrast, the aluminum species in PACl-70d hydrolyzed relatively slowly and grew a little
432 slower at a sulfate concentration of 6.4 mg-SO_4^{2-}/L (Water E3). They barely hydrolyzed
433 without sulfate ions and did not grow larger than 10 μm (Water E1). They grew rapidly at
434 a sulfate concentration of 15.8 mg/L (Waters E4 and E5). Although the concentrations of
435 Na^+ and Mg^{2+} differ in Waters E4 and E5, the rates of the hydrolysis were about the same.
436 The aluminum species in PACl-70t grew very slowly, even at a sulfate concentration of
437 15.8 mg/L. The growth trend of PACl-70t at a sulfate concentration of 48.8 mg/L was
438 similar to that of PACl-70d at a sulfate concentration of 6.4 mg/L. Therefore, the results
439 indicate that sulfate ions are essential for the hydrolysis of PACl-70d and PAC-70t, and
440 they show that PACl-70t requires a much higher concentration of sulfate for its rapid

441 hydrolysis than PACl-70d.

442 The pattern of hydrolysis rates was similar to the trend of coagulation performance,
443 including floc formation and the concentration of residual particles after CSF. On the
444 other hand, charge neutralization capacity, which was evaluated via the ferron assay and
445 colloid charge, did not explain the different coagulation performances of PACl-70d and
446 PAC-70t, as described in the sections 3.1 and 3.2. Hydrolysis rate rather than charge
447 neutralization capacity, therefore determined coagulation performance. Wang et al. (2002)
448 have reported an enhancement of coagulation performance with increasing SO_4^{2-}/Al ratio
449 in PACl and have explained the SO_4^{2-} effect by a charge neutralization mechanism. Our
450 results are new in terms of two points. First, we focused on SO_4^{2-} in raw water, not in
451 PACl. Second, there were different SO_4^{2-} effect on high-basicity PACls of the same
452 sulfate contents (PACl-70d and PACl-70t) but there was no effect on low-basicity PACl
453 (PACl-50d). Sulfate ion in raw water accelerate hydrolysis of aluminum species in high-
454 basicity PACls, but its mechanism is not cleared yet. A possible mechanism is related to
455 ionic strength and double-layer compression. Sulfate ion in raw water may change charge-
456 neutralization capacity of aluminum species formed after PACl is dosed into raw water.
457 These require further study.

458 Moderately polymerized aluminum species with MWs ranging from 1 to 10 kDa were
459 observed in PACl-70t. These moderately polymerized species may have been related to
460 the distinctive hydrolysis of PACl-70t. PACl-70d contained a high percentage of highly
461 polymerized species with MWs >10 kDa. Among the three PACls, PACl-50d had the
462 highest percentage of species with molecular weights <1 kDa, including monomer Al. We
463 hypothesized that the resistance to hydrolysis was strong for moderately polymerized
464 species followed by highly polymerized species. PACl-70t was produced through a high-

temperature (90–95 °C) process, whereas PACl-70d was prepared through a low-temperature process (<85 °C). PACl-70t contains more sodium and chloride ions per aluminum than PACl-70d (Table 1S). The production temperature and/or salt content, in addition to basicity, may therefore determine hydrolysis resistance and coagulation ability.

4. Conclusion

This study comprehensively investigated the difference between PACl-70d ($Al(OH)_3$-dissolution PACl) and PACl-70t ($AlCl_3$-titration PACl) as well as the difference between PACl-70d (high-basicity PACl) and PACl-50d (normal-basicity PACl) in terms of their coagulation ability to form floc particles and to reduce the concentration of SPAC particles in CSF-treated water.

The coagulation performance of PACl-70d was superior to that of PACl-70t, although the ferron distribution, colloid charge, and sulfate ion content were the same. Charge neutralization capacities were likewise sufficient for PACl-70t and PACl-70d, but the very low hydrolysis of aluminum species in PACl-70t versus PACl-70d resulted in poor floc formation by the former.

PACl-70d was superior to PACl-50d in reducing residual carbon particles after CSF, although the rate of floc particle formation was somewhat slower for PACl-70d than for PACl-50d. The similarities of the residual turbidities after coagulation sedimentation could have been due to the high charge neutralization capacity of PACl-70d. However, sulfate ion was required in raw water for PACl-70d to be effective.

When the raw water contained very low concentrations of sulfate ions, the aluminum species in PACl-70d hydrolyzed very slowly and did not form floc particles. In contrast,

PACl-50d did not need sulfate ions. Finally, PACl-70d was inferior to PACl-50d when sulfate ion concentrations in raw water were very low.

The three PACls were clearly different in terms of their MW distributions and their *m*/*z* values determined by ESI-MS, but they did not necessarily differ based on the ferron assay. Polymerized aluminum species, in particular those with MWs of 1–10 kDa, might be highly resistant to hydrolysis and may require sulfate ions for hydrolysis and for effective coagulation.

Hydrolysis of aluminum species as well as charge neutralization capacity are key determinants of coagulation effectiveness.

Acknowledgments

This work was supported by JSPS (Japan Society for the Promotion of Science) KAKENHI Grant Number JP16H06362. The authors gratefully acknowledge Futamura Chemical for providing PAC samples.

References

Allouche, L., Gérardin, C., Loiseau, T., Férey, G., Taulelle, F., 2002. Al30: A Giant Aluminum Polycation. Angew. Chemie Int. Ed. 39, 511–514. https://doi.org/10.1002/(sici)1521-3773(20000204)39:3<511::aid-anie511>3.0.co;2-n

Ando, N., Matsui, Y., Kurotobi, R., Nakano, Y., Matsushita, T., Ohno, K., 2010. Comparison of natural organic matter adsorption capacities of super-powdered activated carbon and powdered activated Carbon. Water Res. 44, 4127–4136.

513 https://doi.org/10.1016/j.watres.2010.05.029
514 Bonvin, F., Jost, L., Randin, L., Bonvin, E., Kohn, T., 2016. Super-fine powdered
515 activated carbon (SPAC) for efficient removal of micropollutants from wastewater
516 treatment plant effluent. Water Res. 90, 90–99.
517 https://doi.org/10.1016/j.watres.2015.12.001
518 Casey, W.H., 2006. Large aqueous aluminum hydroxide molecules. Chem. Rev. 106, 1–
519 16. https://doi.org/10.1021/cr040095d
520 Chen, Z., Luan, Z., Fan, J., Zhang, Z., Peng, X., Fan, B., 2007. Effect of thermal
521 treatment on the formation and transformation of Keggin Al13 and Al30 species in
522 hydrolytic polymeric aluminum solutions. Colloids Surfaces A Physicochem. Eng.
523 Asp. 292, 110–118. https://doi.org/10.1016/j.colsurfa.2006.06.005
524 Chu, Y., Gao, B., Yue, Q., Wang, Y., 2008. Investigation of dynamic processing on
525 aluminum floc aggregation: Cyclic shearing recovery and effect of sulfate ion. Sci.
526 China, Ser. B Chem. 51, 386–392. https://doi.org/10.1007/s11426-007-0129-2
527 De Hek, H., Stol, R.J., De Bruyn, P.L., 1978. Hydrolysis-precipitation studies of
528 aluminum(III) solutions. 3. The role of the sulfate ion. J. Colloid Interface Sci. 64,
529 72–89. https://doi.org/10.1016/0021-9797(78)90336-3
530 Feng, C., Tang, H., Wang, D., 2007. Differentiation of hydroxyl-aluminum species at
531 lower OH/Al ratios by combination of 27Al NMR and Ferron assay improved with
532 kinetic resolution. Colloids Surfaces A Physicochem. Eng. Asp. 305, 76–82.
533 https://doi.org/10.1016/j.colsurfa.2007.04.043
534 Gao, B., Yue, Q., 2005. Effect of SO42-/Al3+ratio and O-/Al3+value on the
535 characterization of coagulant poly-aluminum-chloride-sulfate (PACS) and its
536 coagulation performance in water treatment. Chemosphere 61, 579–584.

https://doi.org/10.1016/j.chemosphere.2005.03.013

Japanese Industrial Standards Committee, 1996. Poly aluminum chloride for water works. URL https://www.jisc.go.jp/app/jis/general/GnrJISNumberNameSearchList?toGnrJISStandardDetailList

Kimura, M., Matsui, Y., Kondo, K., Ishikawa, T.B., Matsushita, T., Shirasaki, N., 2013. Minimizing residual aluminum concentration in treated water by tailoring properties of polyaluminum coagulants. Water Res. 47, 2075–2084. https://doi.org/10.1016/j.watres.2013.01.037

Kimura, M., Matsui, Y., Saito, S., Takahashi, T., Nakagawa, M., Shirasaki, N., Matsushita, T., 2015. Hydraulically irreversible membrane fouling during coagulation-microfiltration and its control by using high-basicity polyaluminum chloride. J. Memb. Sci. 477, 115–122. https://doi.org/10.1016/j.memsci.2014.12.033

Letterman, R.D., Yiacoumi, S., 2010. Coagulation and flocculation, in: Edzwald, J.K. (Ed.), Water Quality and Treatment A Handbook on Drinking Water. McGrawHill, pp. 8.1-8.81.

Matsui, Y., Ishikawa, T.B., Kimura, M., Machida, K., Shirasaki, N., Matsushita, T., 2013a. Aluminum concentrations of sand filter and polymeric membrane filtrates: A comparative study. Sep. Purif. Technol. 119, 58–65. https://doi.org/10.1016/j.seppur.2013.09.006

Matsui, Y., Murase, R., Sanogawa, T., Aoki, N., Mima, S., Inoue, T., Matsushita, T., 2004. Micro-ground powdered activated carbon for effective removal of natural organic matter during water treatment. Water Sci. Technol. Water Supply 4, 155–

163. https://doi.org/10.2166/ws.2004.0073

Matsui, Y., Nakao, S., Sakamoto, A., Taniguchi, T., Pan, L., Matsushita, T., Shirasaki, N., 2015. Adsorption capacities of activated carbons for geosmin and 2-methylisoborneol vary with activated carbon particle size: Effects of adsorbent and adsorbate characteristics. Water Res. 85, 95–102. https://doi.org/10.1016/j.watres.2015.08.017

Matsui, Y., Nakao, S., Taniguchi, T., Matsushita, T., 2013b. Geosmin and 2-methylisoborneol removal using superfine powdered activated carbon: Shell adsorption and branched-pore kinetic model analysis and optimal particle size. Water Res. 47, 2873–2880. https://doi.org/10.1016/j.watres.2013.02.046

Matsui, Y., Shirasaki, N., Yamaguchi, T., Kondo, K., Machida, K., Fukuura, T., Matsushita, T., 2017. Characteristics and components of poly-aluminum chloride coagulants that enhance arsenate removal by coagulation: Detailed analysis of aluminum species. Water Res. 118, 177–186. https://doi.org/10.1016/j.watres.2017.04.037

Matsui, Y., Yoshida, T., Nakao, S., Knappe, D.R.U., Matsushita, T., 2012. Characteristics of competitive adsorption between 2-methylisoborneol and natural organic matter on superfine and conventionally sized powdered activated carbons. Water Res. 46, 4741–4749. https://doi.org/10.1016/j.watres.2012.06.002

Nakamura, H., 2009. FT-NMR data processing by computer, Secong edi. ed. Sankyo Shuppan.

Nakazawa, Y., Matsui, Y., Hanamura, Y., Shinno, K., Shirasaki, N., Matsushita, T., 2018a. Minimizing residual black particles in sand filtrate when applying super-fine powdered activated carbon: Coagulants and coagulation conditions. Water

585 Res. 147, 311–320. https://doi.org/10.1016/j.watres.2018.10.008
586 Nakazawa, Y., Matsui, Y., Hanamura, Y., Shinno, K., Shirasaki, N., Matsushita, T.,
587 2018b. Identifying, counting, and characterizing superfine activated-carbon
588 particles remaining after coagulation, sedimentation, and sand filtration. Water
589 Res. 138, 160–168. https://doi.org/10.1016/j.watres.2018.03.046
590 Pan, L., Nishimura, Y., Takaesu, H., Matsui, Y., Matsushita, T., Shirasaki, N., 2017.
591 Effects of decreasing activated carbon particle diameter from 30 Mm to 140 nm on
592 equilibrium adsorption capacity. Water Res. 124, 425–434.
593 https://doi.org/10.1016/j.watres.2017.07.075
594 Parker, D.R., Bertsch, P.M., 1992. Identification and Quantification of the “Al13”
595 Tridecameric Aluminum Polycation Using Ferron. Environ. Sci. Technol. 26, 908–
596 914. https://doi.org/10.1021/es00029a006
597 Partlan, E., Davis, K., Ren, Y., Apul, O.G., Mefford, O.T., Karanfil, T., Ladner, D.A.,
598 2016. Effect of bead milling on chemical and physical characteristics of activated
599 carbons pulverized to superfine sizes. Water Res. 89, 161–170.
600 https://doi.org/10.1016/j.watres.2015.11.041
601 Sato, F., Matsuda, S., 2009. Novel Basic Aluminum Chloride, Its Manufacturing
602 Method and Its Application. Japanese Patent, Appl.
603 Sposito, G., 1995. The Environmental Chemistry of Aluminum, Second Edition. Taylor
604 & Francis.
605 Sricharoenchaikit, P., Letterman, R.D., 1987. EFFECT OF AL(III) AND SULFATE
606 ION ON FLOCCULATION KINETICS. J. Environ. Eng. -ASCE 113, 1120–1138.
607 https://doi.org/10.1061/(ASCE)0733-9372(1987)113:5(1120)
608 Tang, H., Xiao, F., Wang, D., 2015. Speciation, stability, and coagulation mechanisms

609 of hydroxyl aluminum clusters formed by PACl and alum: A critical review. Adv.
610 Colloid Interface Sci. 226, 78–85. https://doi.org/10.1016/j.cis.2015.09.002
611 Wang, D., Sun, W., Xu, Y., Tang, H., Gregory, J., 2004. Speciation stability of
612 inorganic polymer flocculant-PACl. Colloids Surfaces A Physicochem. Eng. Asp.
613 243, 1–10. https://doi.org/10.1016/j.colsurfa.2004.04.073
614 Wang, D., Tang, H., Gregory, J., 2002. Relative importance of charge neutralization and
615 precipitation on coagulation of kaolin with PACI: Effect of sulfate ion. Environ.
616 Sci. Technol. 36, 1815–1820. https://doi.org/10.1021/es001936a
617 Yan, M., Wang, D., Ni, J., Qu, J., Chow, C.W.K., Liu, H., 2008. Mechanism of natural
618 organic matter removal by polyaluminum chloride: Effect of coagulant particle size
619 and hydrolysis kinetics. Water Res. 42, 3361–3370.
620 https://doi.org/10.1016/j.watres.2008.04.017
621 Yan, M., Wang, D., Qu, J., He, W., Chow, C.W.K., 2007. Relative importance of
622 hydrolyzed Al(III) species (Ala, Alb, and Alc) during coagulation with
623 polyaluminum chloride: A case study with the typical micro-polluted source
624 waters. J. Colloid Interface Sci. 316, 482–489.
625 https://doi.org/10.1016/j.jcis.2007.08.036
626 Ye, C., Wang, D., Shi, B., Yu, J., Qu, J., Edwards, M., Tang, H., 2007. Alkalinity effect
627 of coagulation with polyaluminum chlorides: Role of electrostatic patch. Colloids
628 Surfaces A Physicochem. Eng. Asp. 294, 163–173.
629 https://doi.org/10.1016/j.colsurfa.2006.08.005
630

Table 1

Ion components, alkalinity, and DOC of waters used in this study.

Series	Water	Na^+	K^+	Mg^{2+}	Ca^{2+}	Cl^-	NO_3^-	SO_4^{2-}	Alkalinity	DOC	Source
		mg/L	mg/L	mg/L	mg/L	mg/L	mg/L	mg/L	mg-$CaCO_3$/L	mg/L	
C Series	C0	13.8	1.7	4.5	5.8	11.9	0.3	18.8	27	2.4	Chibaberi River
	C1	33.0	1.7	4.3	5.7	14.4	0.0	15.9	50	0.9	
	C2	28.3	1.7	4.5	5.7	21.6	0.0	6.4	50	NM	
E Series	E1	24.2	0.6	0.0	12.5	22.5	0.9	0.0	50	NM	Elix water
	E2	24.1	0.5	0.6	12.3	22.1	0.9	3.5	50	NM	
	E3	24.0	0.6	1.3	12.5	22.3	1.0	6.4	50	NM	
	E4	25.3	0.5	3.9	12.5	25.7	1.1	15.8	50	NM	
	E5	30.5	0.6	0.0	12.5	22.1	0.9	15.7	50	NM	
	E6	20.5	0.5	6.1	12.3	25.3	1.0	28.2	50	NM	
	E7	21.0	0.5	10.2	12.3	25.7	1.0	48.8	50	NM	
J Series	J1	1.9	0.4	0.9	6.6	1.7	0.6	4.0	16	0.5	Joganji River
	J2	8.0	0.4	0.9	6.6	1.7	0.6	15.3	16	0.5	

(NM: Not measured, DOC: dissolved organic carbon)

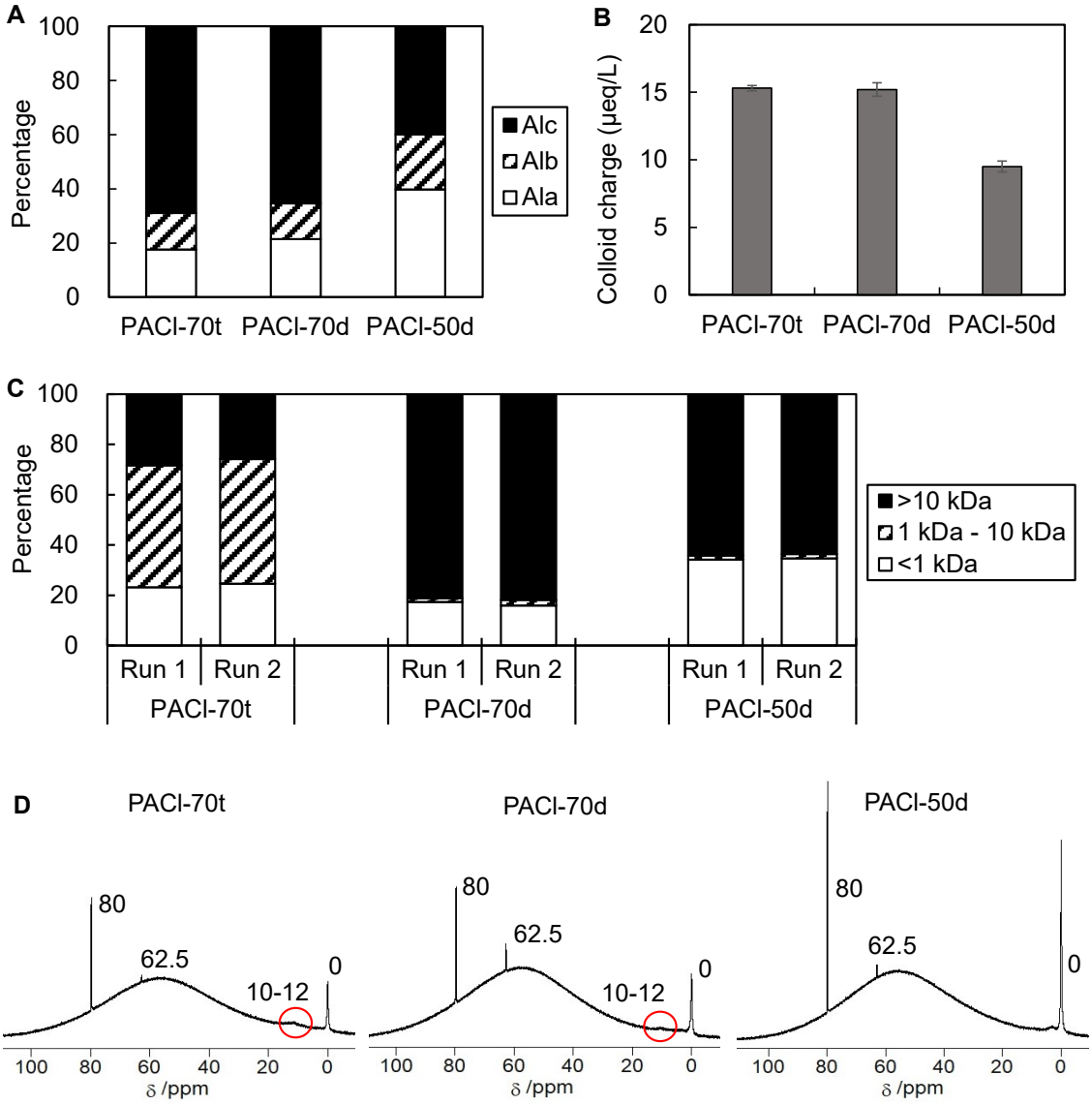

Fig. 1. Characteristics of PACl-70t, PACl-70d, and PACl-50d. Panel A: ferron distributions. Panel B: colloid charges. Panel C: molecular weight distribution of aluminum species (This experiment was conducted twice at the same condition. Panel D: of ^{27}Al-NMR spectra (The peaks at δ = 80 ppm are due to the internal standard, $NaAl(OH)_4$. The red circles indicate broad peaks at δ = 10-12 ppm).

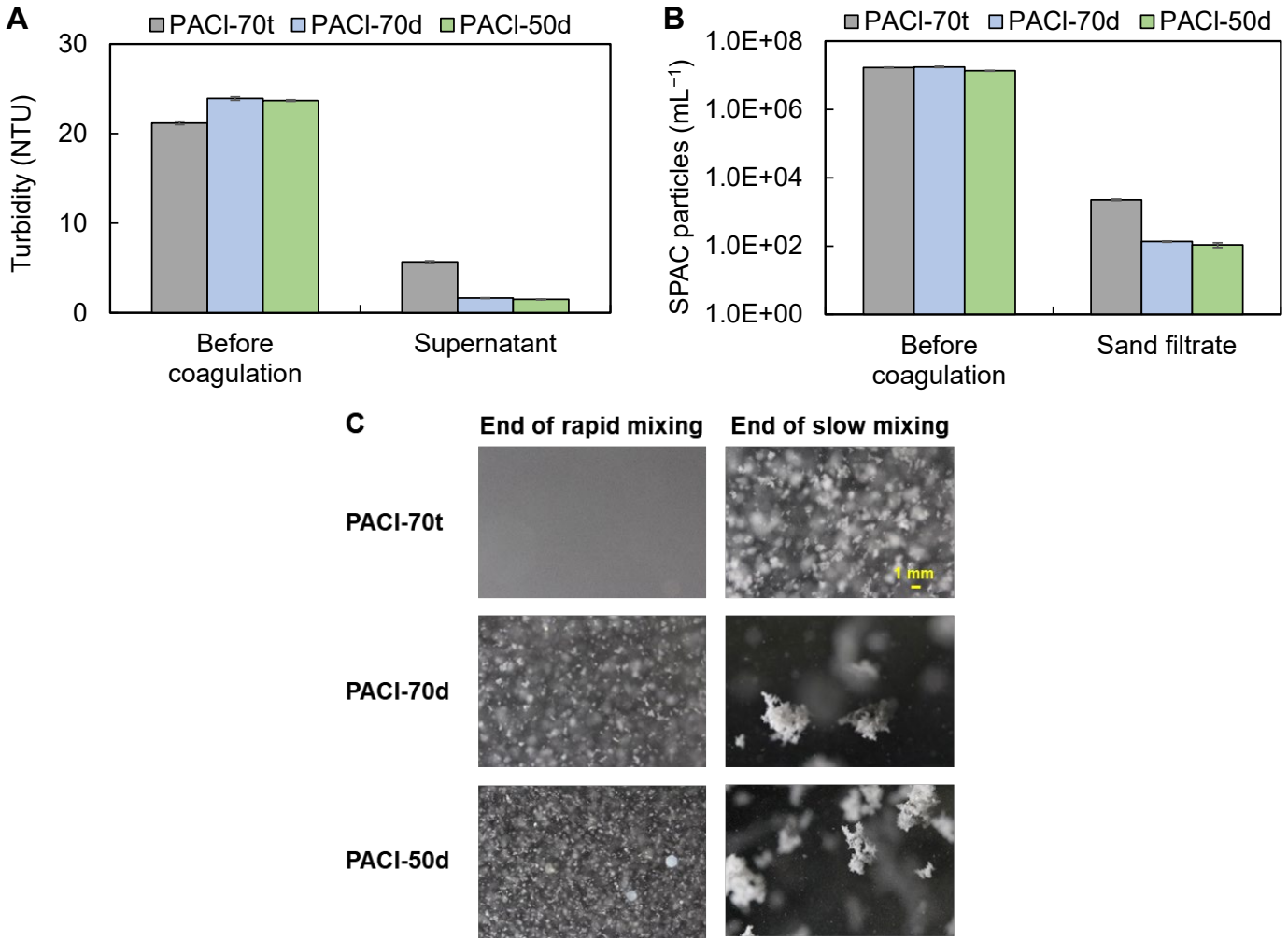

Fig. 2. Turbidity in supernatant (Panel A), residual SPAC particles in sand filtrate (Panel B), and photographs taken at the ends of rapid mixing and slow mixing (Panel C). Water C1 was used. Initial SPAC concentration was 2 mg/L. PACl-70t, PACl-70d, and PACl-50d were used at a dosage of 2.5 mg-Al/L. Coagulation pH was 7.0. Turbidities of sand filtrates were also measured, but they were very low: <0.1 NTU.

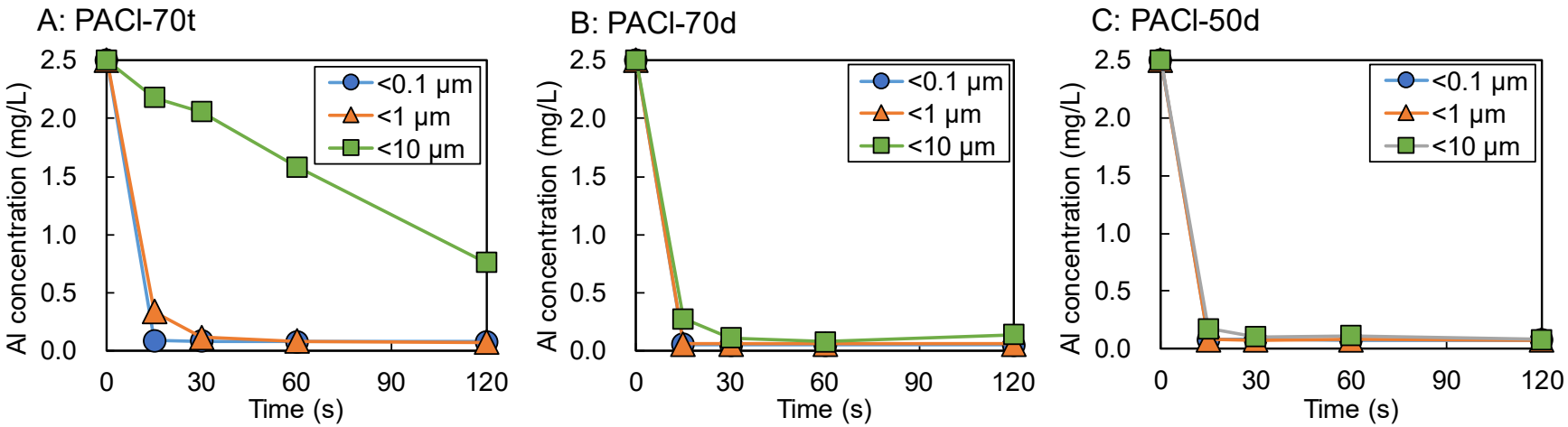

Fig. 3. Rate of hydrolysis of PACl-70t (Panel A), PACl-70d (Panel B), and PACl-50d (Panel C). Water E4 was used. PACl-70t, PACl-70d, and PACl-50d were used at a dosage of 2.5 mg-Al/L. Coagulation pH was 7.0.

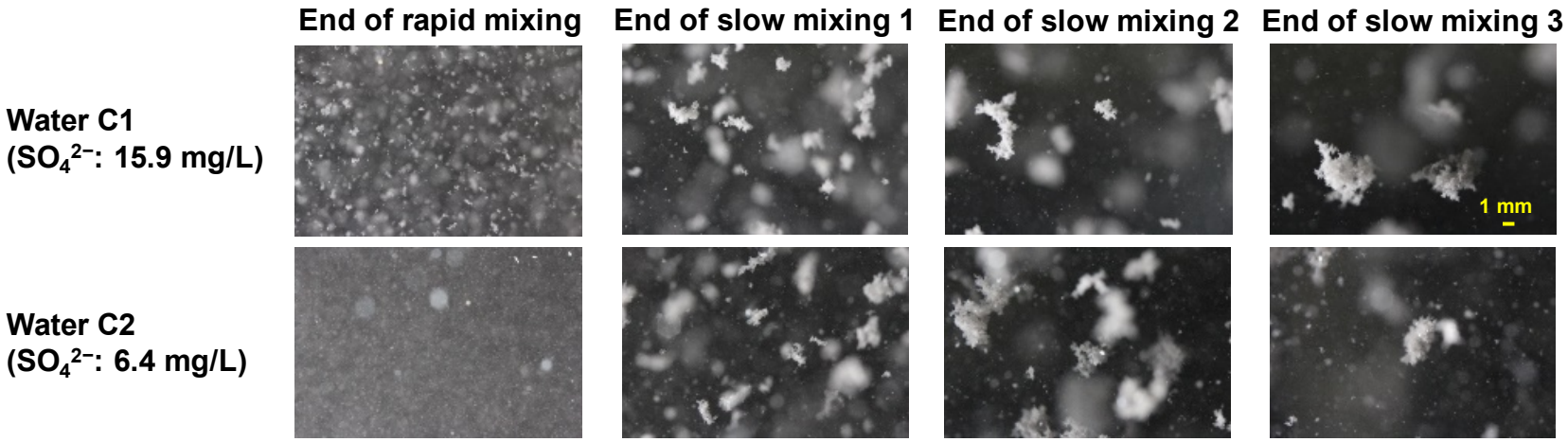

Fig. 4. Photographs taken at the end of rapid mixing and each slow mixing stage. Waters C1 (upper pictures) and C2 (lower pictures), including SO_4^{2-} concentrations of 15.9 and 6.4 mg/L, respectively, were used. Initial SPAC concentration was 2 mg/L. PACl-70d was used at a dosage of 2.5 mg-Al/L. Coagulation pH was 7.0.

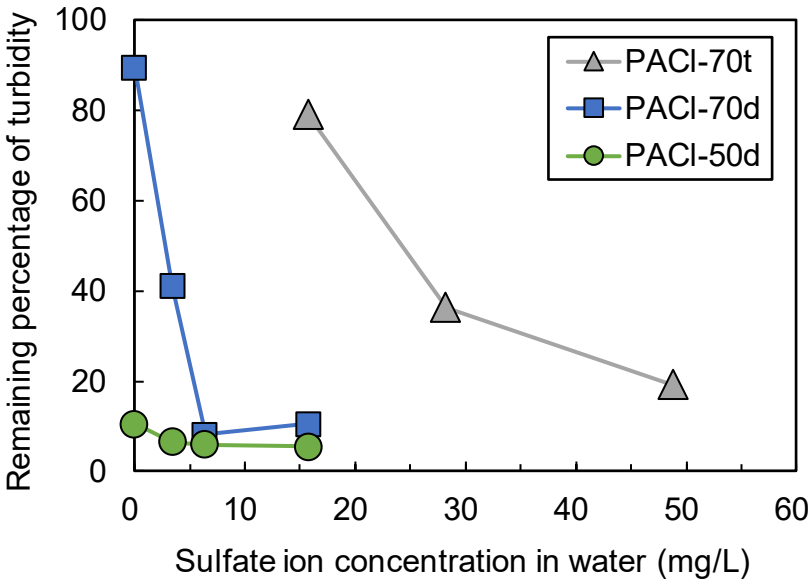

Fig. 5. Plots of the percentage of turbidity remaining after coagulation and sedimentation against sulfate ion concentration in raw water. Waters E1–4 and E6-7 were used. Initial SPAC concentration was 2 mg/L. PACl-70t, PACl-70d, and PACl-50d were used at a dosage of 2.5 mg-Al/L. Coagulation pH was 7.0.

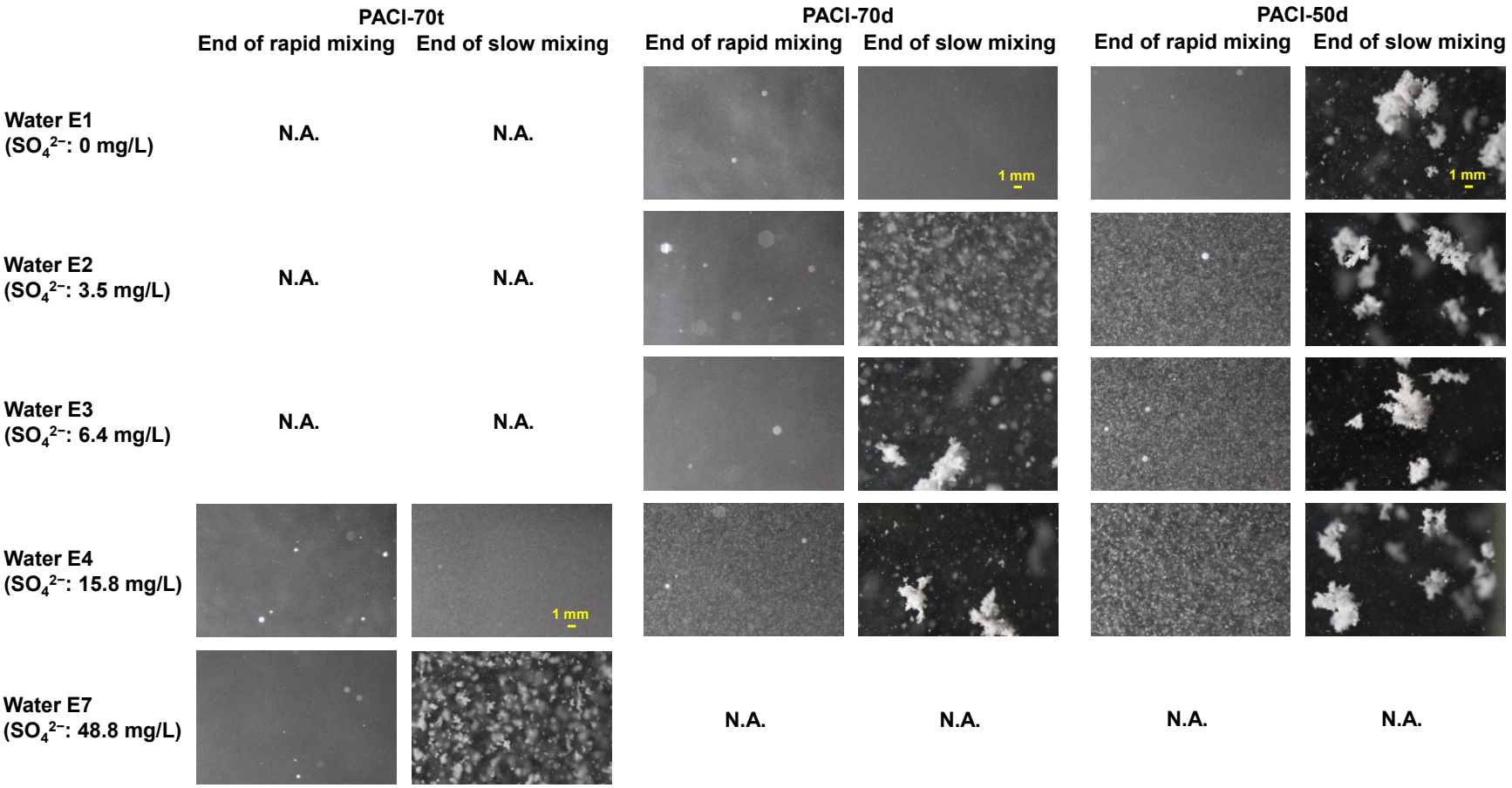

Fig. 6. Photographs taken at the end of slow mixing. Waters E1, 2, 3, 4, and 7 were used. Initial SPAC concentration was 2 mg/L. PACl-70t, PACl-70d, and PACl-50d were used at a dosage of 2.5 mg-Al/L. Coagulation pH was 7.0. All the pictures during slow mixing are shown in Fig. 6S, Fig. 7S, and Fig. 8S in the SI.

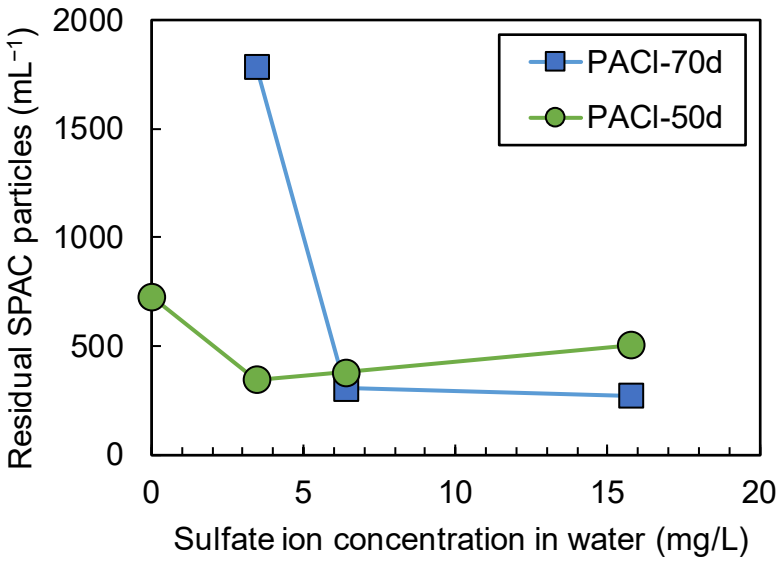

Fig. 7. Plots of residual SPAC particle concentration in sand filtrate against sulfate concentration in raw water. Waters E1, E2, E3, and E4 with sulfate ion concentrations of 0.0, 6.4, 15.8, and 28.2 mg/L, respectively, were used. Initial SPAC concentration was 2 mg/L. PACl dosage was 2.5 mg-Al/L. Coagulation pH was 7.0.

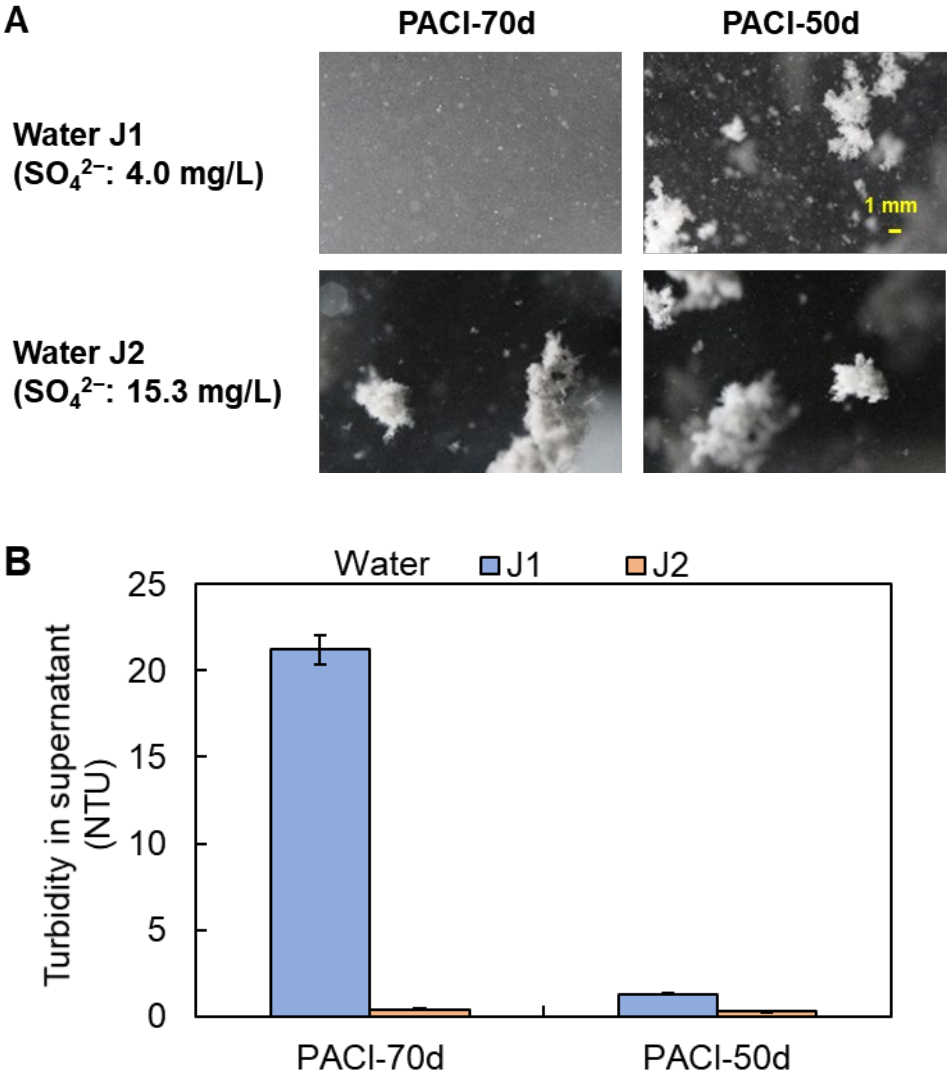

Fig. 8. Photographs taken at the end of slow mixing 3 (Panel A) and residual turbidities of supernatants (Panel B). Waters J1 and J2 with different sulfate ion concentrations of 4.0 and 15.3 mg/L, respectively, were used. Initial SPAC concentration was 2 mg/L. PACl-70d and PACl-50d were used at a dosage of 4.0 mg-Al/L. Coagulation pH was 7.0.

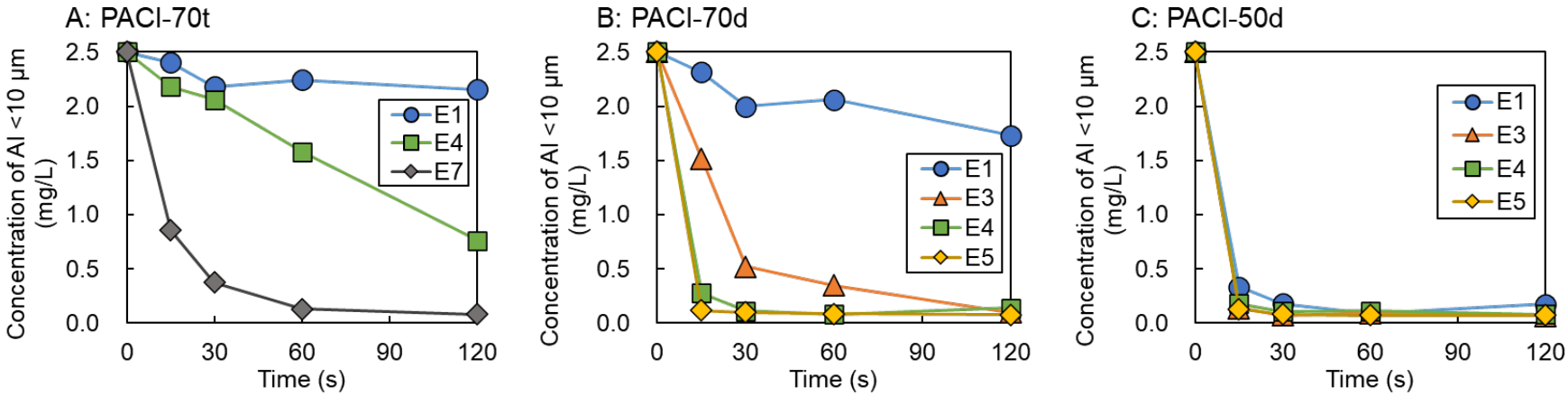

Fig. 9. Change of concentration of aluminum that passed through a membrane with a 10-µm pore size. Waters E1, E3, E4, E5, and E7 with sulfate ion concentrations of 0.0, 6.4, 15.8, 15.7, and 48.8 mg/L, respectively, were used. PACl-70t (Panel A), PACl-70d (Panel B), and PACl-50d (Panel C) were dosed at 2.5 mg-Al/L. pH during mixing was 7.

Highlights

- High-basicity PACl, esp. that made by $AlCl_3$-titration, is resistant to hydrolysis.
- $AlCl_3$-titration PACl is inferior to $Al(OH)_3$-dissolution PACl due to slow hydrolysis.
- Sulfate ions in raw water affect the performance of high-basicity PACl.
- High-basicity PACl requires sulfate ions, but normal-basicity PACl does not.
- Hydrolysis and charge neutralization capacity are both needed for coagulation.

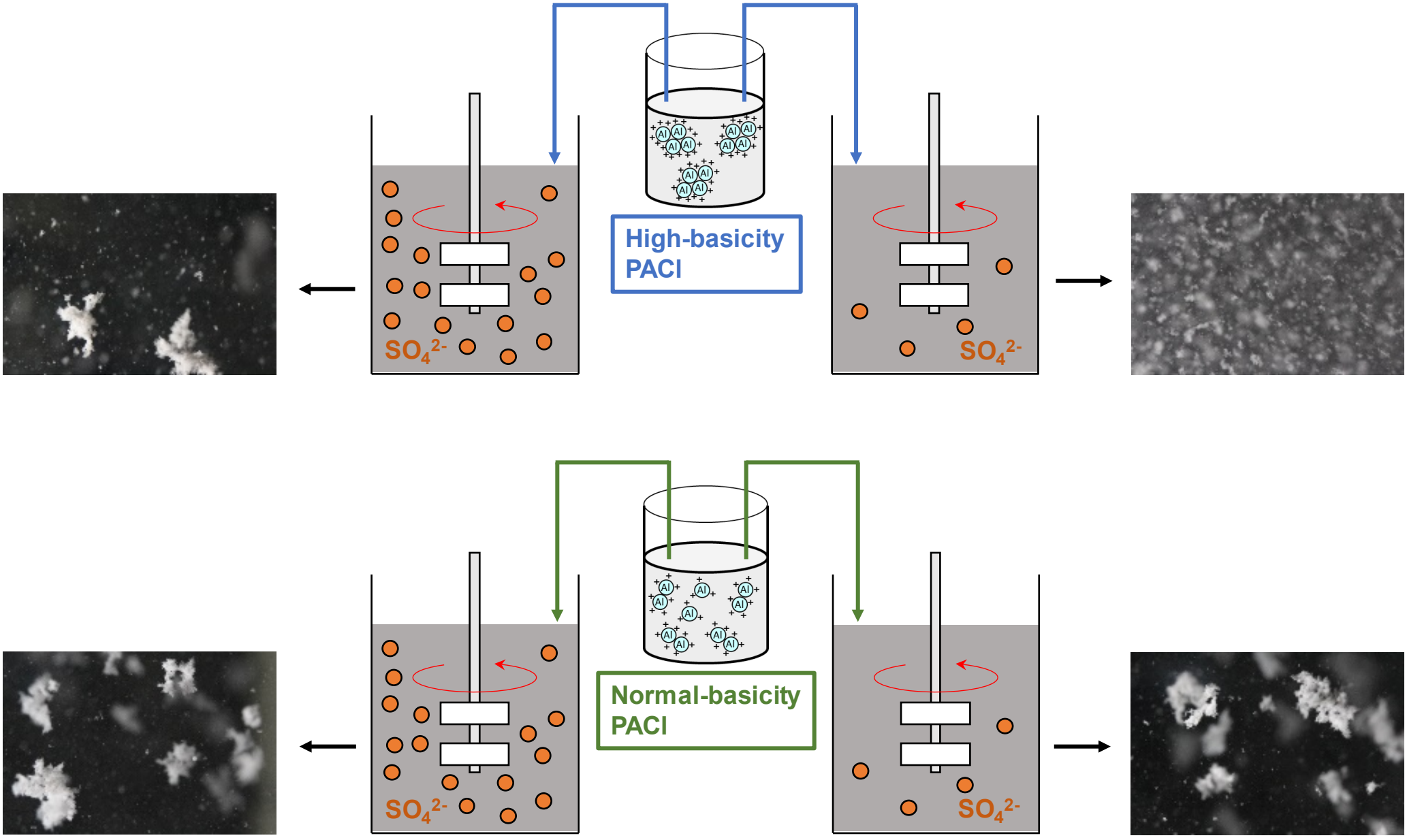
High-basicity
PACI
SO_4^{2-}
SO_4^{2-}
Normal-basicity
PACI
SO_4^{2-}
SO_4^{2-}

Supplementary Information

Sulfate ion in raw water affects performance of high-basicity PACl coagulants produced by Al(OH)3 dissolution and base-titration: removal of SPAC particles by coagulation-flocculation, sedimentation, and sand filtration

Yize Chen [a], Yoshifumi Nakazawa [a], Yoshihiko Matsui [b, *], Nobutaka Shirasaki [b], Taku Matsushita [b]

[a] Graduate School of Engineering, Hokkaido University.
N13W8 Sapporo 060-8628 Japan

[b] Faculty of Engineering, Hokkaido University
N13W8 Sapporo 060-8628 Japan

* Corresponding author. Phone: +81-11-706-7280.
E-mail address: matsui@eng.hokudai.ac.jp (Y. Matsui)

Table 1S

Properties of the PACls used in this study.

	PACl-70t	PACl-70d	PACl-50d
Al content (mol/L)	0.1	2.5	2.5
SO_4^{2-}/Al (mole ratio)	0.11	0.11	0.14
Na^+/Al (mole ratio)	2.18	0.27	0.00
Cl^-/Al (mole ratio)	3.86	1.04	1.25
Basicity (%)	69.6	68.1	50.6

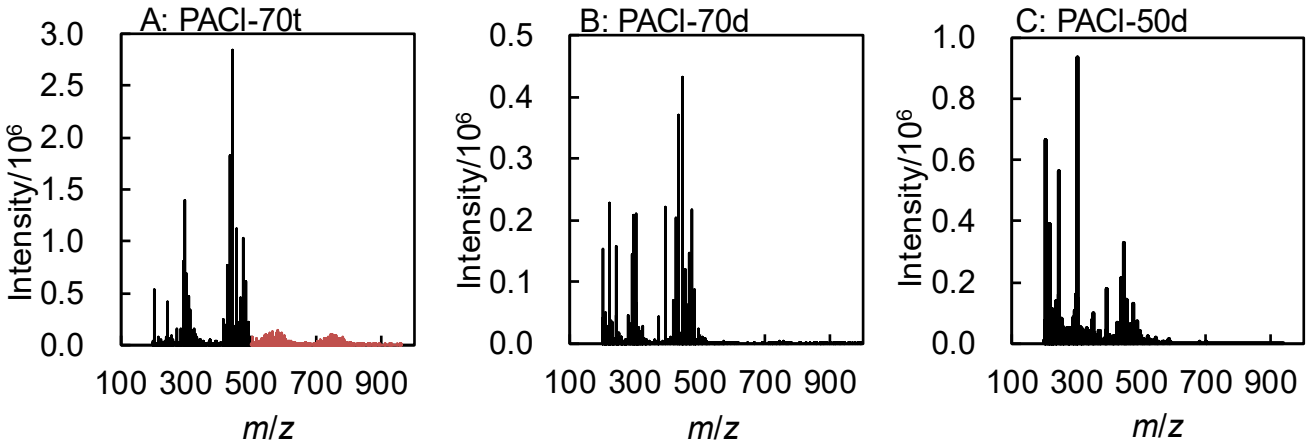

Fig. 1S. ESI-MS spectra of PACl-70t, PACl-70d, and PACl-50d.

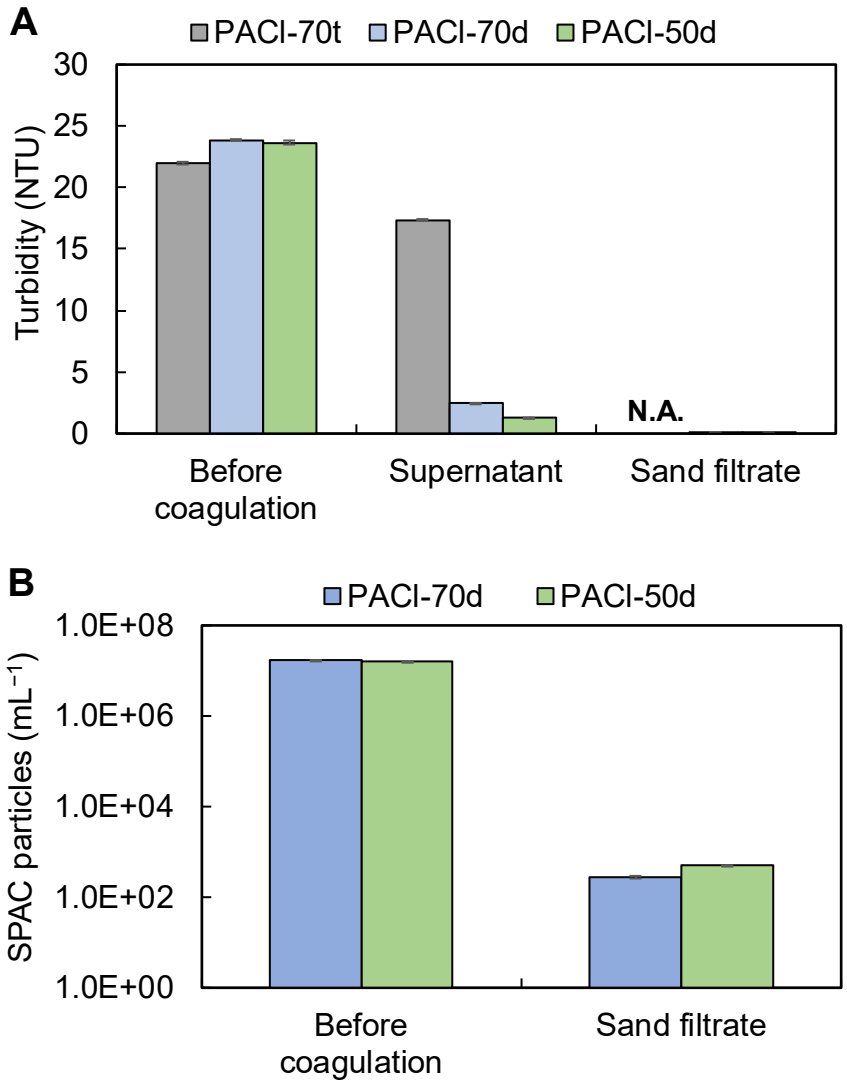

Fig. 2S. Turbidity in supernatant and sand filtrate (Panel A) and residual SPAC particles in sand filtrate (Panel B). Water E4 was used. Initial SPAC concentration was 2 mg/L. PACl-70t, PACl-70d, and PACl-50d were used with the dosage of 2.5 mg-Al/L. Coagulation pH was 7.0. The sand filtration was not conducted for PACl-70t, so the turbidity in sand filtrate of PACl-70t was not available (N.A.).

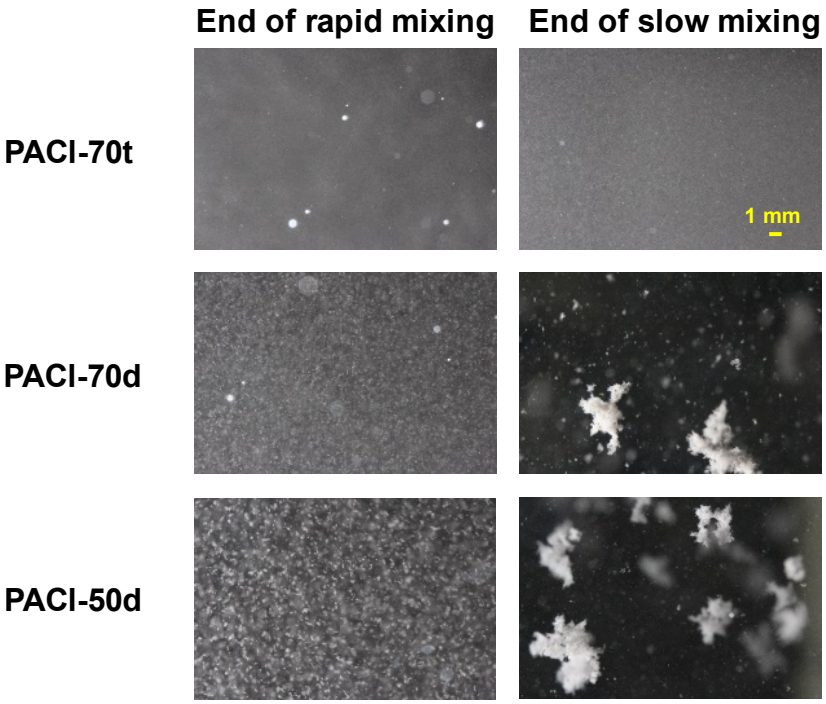

Fig. 3S. Photographs taken at the end of rapid mixing and slow mixing. Water E4 was used. Initial SPAC concentration was 2 mg/L. PACl-70t, PACl-70d, and PACl-50d were used at a dosage of 2.5 mg-Al/L. Coagulation pH was 7.0.

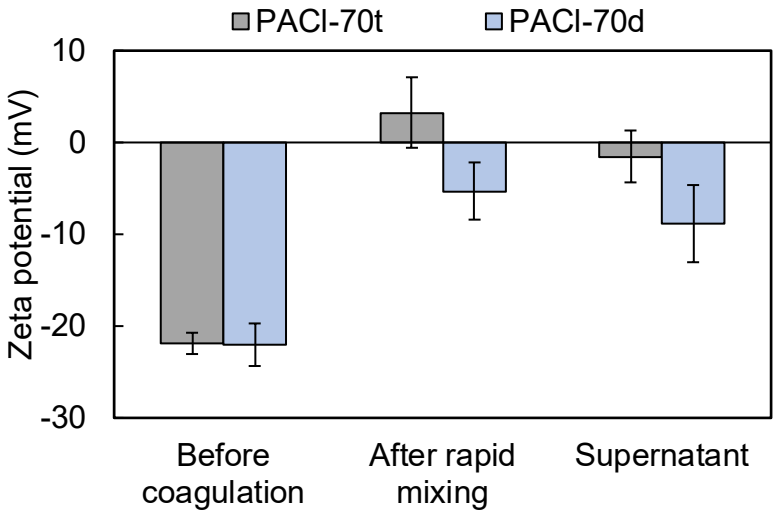

Fig. 4S. Change of zeta potential during CSF experiment. Water C1 was used. Initial SPAC concentration was 2 mg/L. PACl-70t and PACl-70d were used at a dosage of 2.5 mg-Al/L. Coagulation pH was 7.0.

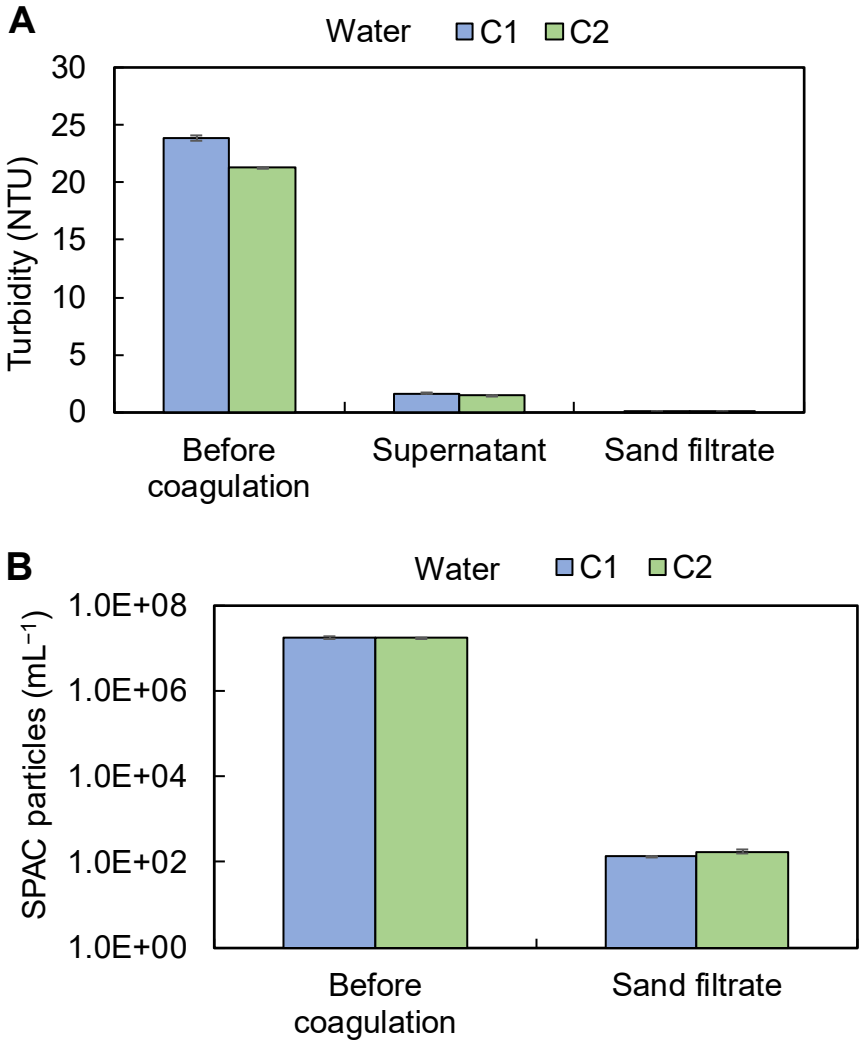

Fig. 5S. Changes of turbidity (Panel A) and SPAC-particle number concentration (Panel B) during CSF. Waters C1 (SO_4^{2-} 15.9 mg/L) and C2 (SO_4^{2-} 6.4 mg/L) were used. Initial SPAC concentration was 2 mg/L. PACl-70d was used at a dosage of 2.5 mg-Al/L. Coagulation pH was 7.0.

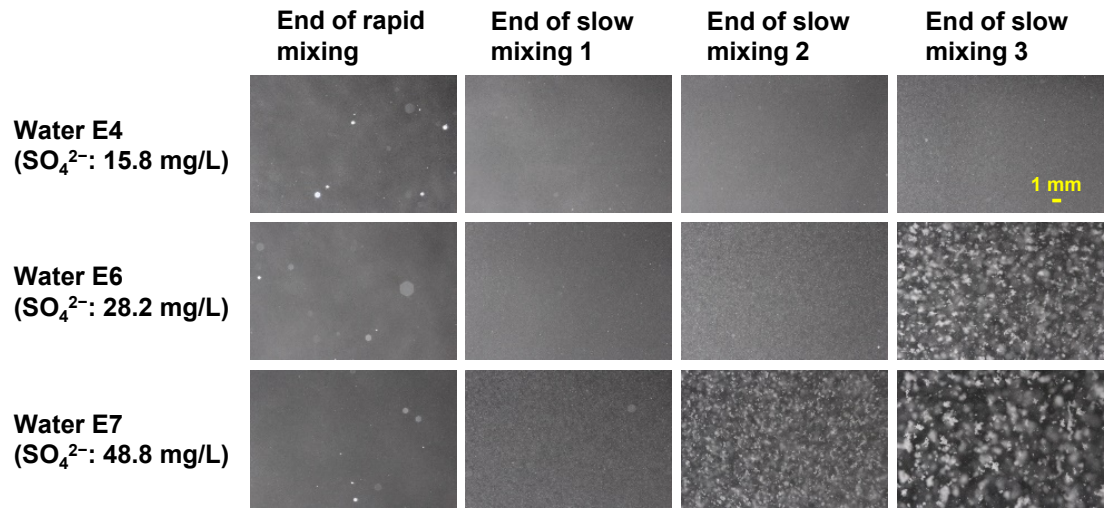

Fig. 6S. Photographs taken at the ends of rapid mixing, slow mixing 1, slow mixing 2, and slow mixing 3. Waters E4, E6 and E7 with sulfate ion concentrations of 15.8, 28.2, and 48.8 mg/L, respectively, were used. Initial SPAC concentration was 2 mg/L. PACl-70t was used at a dosage of 2.5 mg-Al/L. Coagulation pH was 7.0.

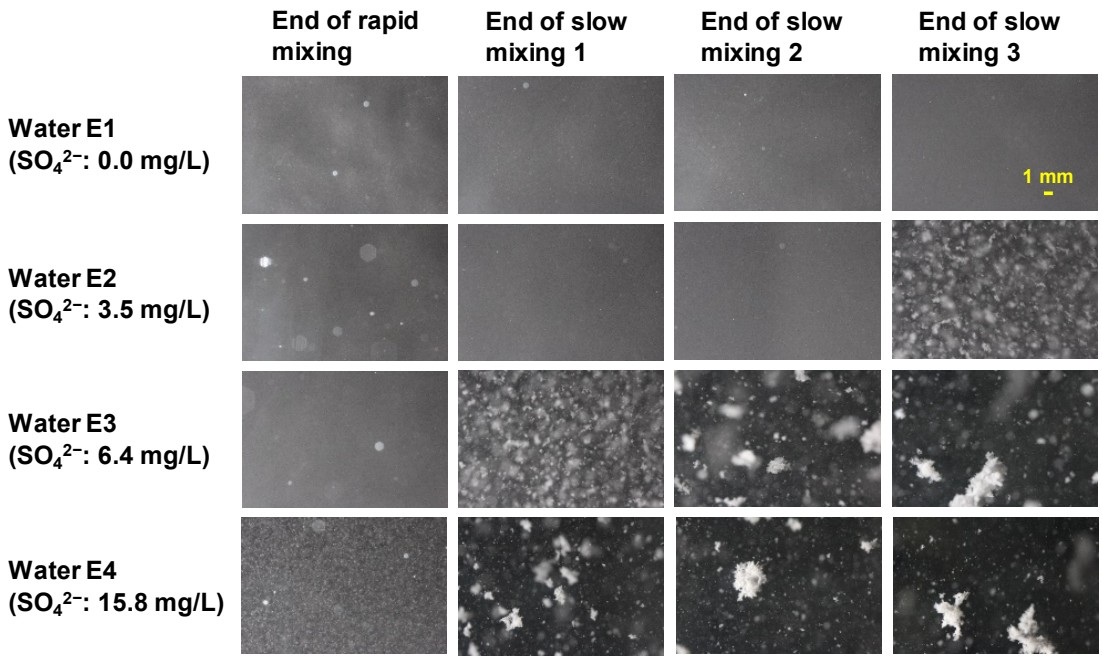

Fig. 7S. Photographs taken at the end of rapid mixing, slow mixing 1, slow mixing 2, and slow mixing 3. Waters E1, E2, E3, and E4 with sulfate ion concentrations of 0.0, 3.5, 6.4 and 15.8 mg/L, respectively, were used. Initial SPAC concentration was 2 mg/L. PACl-70d was used at a dosage of 2.5 mg-Al/L. Coagulation pH was 7.0.

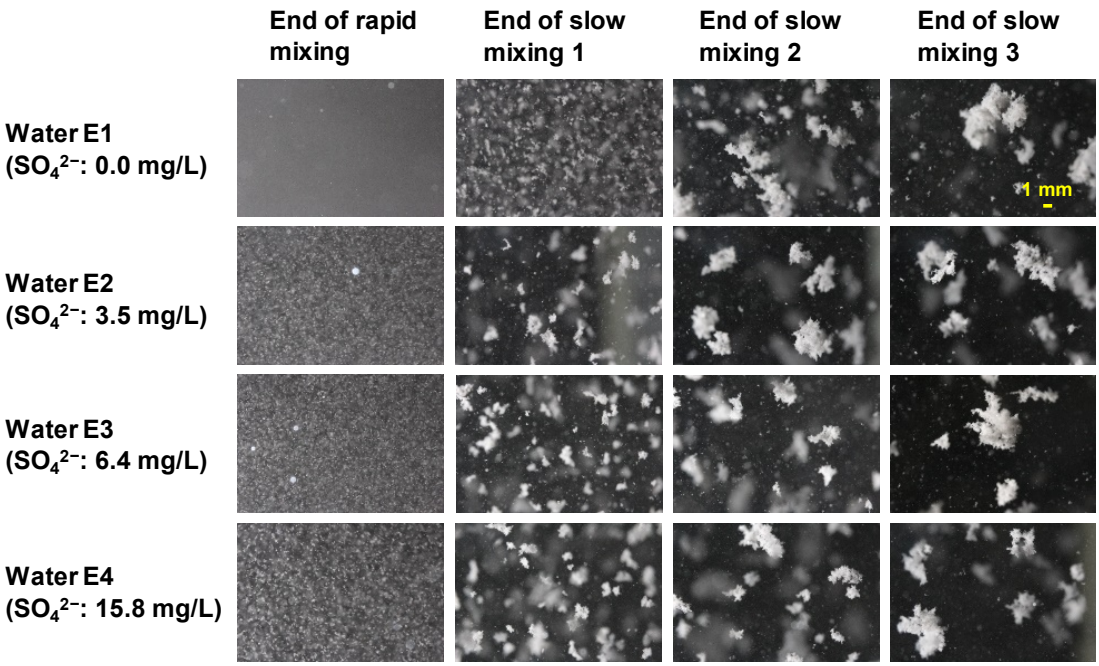

Fig. 8S. Photographs taken at the end of rapid mixing, slow mixing 1, slow mixing 2, and slow mixing 3. Waters E1, E2, E3, and E4 with sulfate ion concentrations of 0.0, 3.5, 6.4 and 15.8 mg/L, respectively, were used. Initial SPAC concentration was 2 mg/L. PACl-50d was used at a dosage of 2.5 mg-Al/L. Coagulation pH was 7.0.

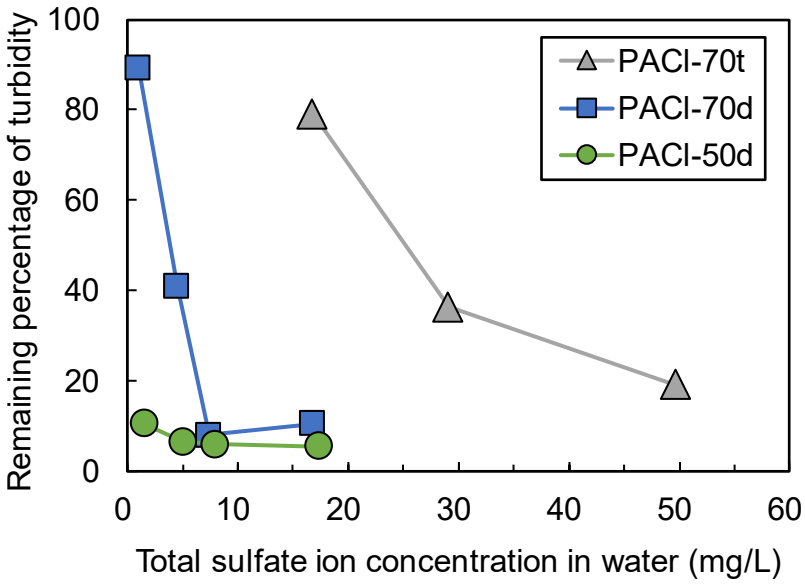

Fig. 9S. Plots of the percentage of turbidity remaining after coagulation and sedimentation against total sulfate ion concentration in raw water. Waters E1–4, and E6–7 with different sulfate ions were used. Initial SPAC concentration was 2 mg/L. PACl-70t, PACl-70d, and PACl-50d were used at a dosage of 2.5 mg-Al/L. Coagulation pH was 7.0.